IJCRT.ORG ISSN : 2320-2882

INTERNATIONAL JOURNAL OF CREATIVE RESEARCH THOUGHTS (IJCRT)

An International Open Access, Peer-reviewed, Refereed Journal

# SPECTROSCOPIC CHARACTERIZATION AND DFT COMPUTATIONAL STUDY FOR THE 4–CHLOROMETHYL PYRIDINE HYDROCHLORIDE MOLECULE

[1*] Keerthana Ravikumar, [2]Soundhariya Segar,[3] Sivaranjini T, [4] Periandy S

[1] Research Scholar,[2]Assistant professor, [3] Assistant Professor, [4]Associate Professor

[1*]Department of Physics,

[1] Kanchi Mamunivar Govt. Institute for Postgraduate studies and research, Pondicherry University, Puducherry, India.

***Abstract:*** In the present study, the structural, optical, and biological properties of the 4–chloromethyl pyridine hydrochloride molecule were examined by quantum computation density functional theory (DFT) using the B3LYP 6-311++G (d,p) basis set. The observed bond length and bond angles were compared with the reported XRD results. HOMO and LUMO orbitals have determined the energy gap. The donor–acceptor interactions are investigated using a second-order Fock matrix. The obtained vibrational frequencies were confirmed with experimental FT-IR and FT-RAMAN analysis. The molecular electrostatic potential surface analysis shows the electrophilic and nucleophilic attack of the present molecule. $^{13}C$ and $^{1}H$ Nuclear Magnetic Resonance data were used to study the molecular structure of the titled molecule at the elemental level. The UV-Vis absorption spectra confirm the optical properties of the titled molecule. The Ramachandran plot of the titled molecule is used to identify the protein's favorable regions for docking. Docking studies confirm the pharmaceutical activity of the titled molecule.

***Keywords:*** *DFT; UV–Vis; HOMO-LUMO; NMR; Molecular Docking*

## I. INTRODUCTION

Pyridine is an aromatic amine with delocalized electron pairs similar to benzene. It is a foul-smelling liquid and it has been widely used for clinical applications [1,2]. Various spectroscopic investigations such as NMR, Raman, IR and UV analysis interpreted its fundamental properties. Pyridine derivatives have a variety of biological properties, including antibacterial, antimicrobial, and anti-diabetic properties. It is used in electrochemical and photochemical processes. Pyridine moieties are commonly employed in medication manufacture due to their basicity and hydrogen bonding capabilities [3]. 4-Chloromethyl pyridine hydrochloride is one of the low-cost pyridine derivatives used in the chemical industry [4]. A detailed quantum computation study by using Density functional theory (DFT) will aid different spectroscopic investigations of the Chloromethyl pyridine hydrochloride molecule [5]. Hence, in this work we investigated the structural, Vibrational, UV, NMR, non-linear optical and thermal properties of

the chloromethyl pyridine hydrochloride molecule using B3LYP functional and 6-311++G(d,p) basis set. To the best of our knowledge, the quantum chemical analysis of the titled compound has not been reported so far.

## II. METHODS

### 2.1 EXPERIMENTAL METHODS

The substance under study, 4-chloromethyl pyridine hydrochloride, was bought from Sigma Aldrich Chemical USA in spectroscopic grade. The FT-IR spectra in the 4000-400 $cm^{-1}$ region were captured using a Bruker IFS 66V spectrometer. The spectral resolution measures around 2 $cm^{-1}$. The FT-Raman spectra of this compound are also captured using the same module with FRA 106 Raman module outfitted with Nd: YAG laser source running at 1.064 m line widths with 200 mW power. The powerful multinuclear FT-NMR model Avance II (Bruker) was used to record the high resolution NMR spectra displayed in Fig.4. The instrument is outfitted with a cryo magnet of field strength 9.4 T with its frequency 400 MHZ for $^{1}H$ and 100 MHZ for $^{13}C$.

### 2.2 Quantum Computational Method

Theoretical approaches and basis sets should be explored in order to achieve both accuracy and computing efficiency requirements. In tackling the electrical structure of molecules, DFT has proven to be quite effective. In this study, the properties of the examined molecule were calculated using the density functional three parameter hybrid model (DFT/B3LYP) at the 6-311G (d,p) and 6-311++G(d,p) basis sets. All calculations were carried out with the GAUSSIAN 09W program package, using the default convergence criteria and no geometry constraints. By using the GAUSSIAN 09W program package, the Raman scattering activities were calculated.

The expression:

$$I_i=10^{-12} \times (V_0-V_i)^4 \times 1 \div V_i \times RA_i \quad \ldots (1)$$

where $I_i$ is the Raman intensity, $RA_i$ is the Raman scattering activities, $V_i$ is the normal mode wave number, and $V_0$ is the excitation laser wave number. The enlarged 6-311++G(d,p) basis set was used to continue computations for the B3LYP functional, which was chosen as the one that yields the most accurate results. The infrared and Raman spectra were interpreted in detail using the results derived at this level of theory.

## III. RESULT

### 3.1 Molecular Geometry

The reactivity, polarity, polarizability, and biological activity of a chemical can all be determined using the structure of the substance. The B3LYP technique with a 6-311++G(d,p) basis set is used to compute the optimal structural characteristics of the target chemical 4- Chloromethyl pyridine Hydrochloride. Fig.1 shows the optimal structure of the chemical with the numbering of atoms. The bond lengths and bond angles estimated for the compound are shown in Table.1. The compound consists of five

C–C bonds, two C–N bonds, one C–Cl bond, and six C-H bonds. Except for C3–C11, which is 1.49Å because of the presence of Cl, all of the CC values are within the predicted range of 1.39Å – 1.40Å [6]. Some of the bond angles are varied C2–C1–N6 (123°), N6–C1–H7 (116°), C1–C2–C3 (118°), C2–C3–C4 (117°), C3–C4–C5 (118°), C4–C5–N6 (123°), C6–C5–H10 (116°), C1–N6–C5 (117°), by the electron-with drawing nature of nitrogen atom and C3–C11–H13 (111°), C3–C11–H14 (111°), C3–C11–Cl12 (111°), Cl12–C11–H13 (105°) and C3–C11–H14 (105°) due to the attachment of chloromethyl group [7] . All the other bond angles are in the $sp^2$ and $sp^3$ hybridization.

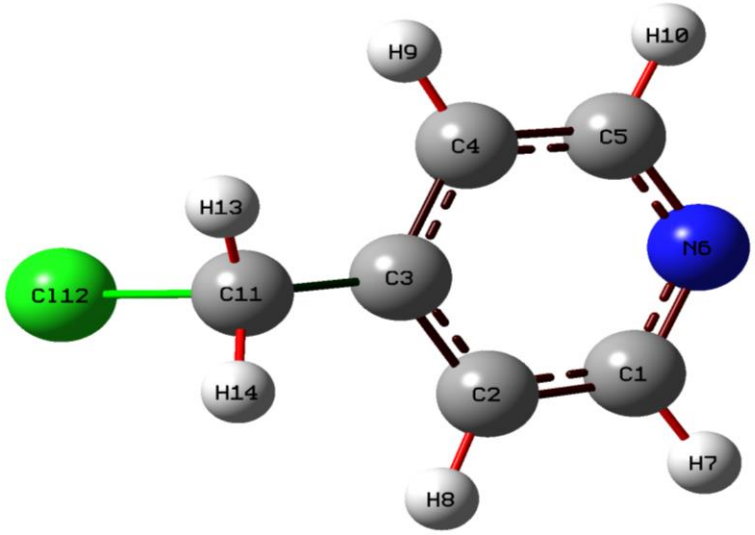


**Fig.1** Optimized molecular structure for 4- Chloromethyl pyridine Hydrochloride

**Table 1** Optimized Geometrical parameter for 4clmpyhycl Computed at B3LYP/6-311++G(d,p).

| **Bond Length** | **B3LYP/ 6-311++G (d,p)** | **Bond Angle ( )** | **B3LYP/ 6-311++G (d,p)** | **Dihedral Angle ( )** | **B3LYP/ 6-311++G (d,p)** |
|---|---|---|---|---|---|
| C1–C2 | 1.3926 | C2–C1–N6 | 123.635 | N6-C1-C2-C3 | 0.0383 |
| C1–N6 | 1.3364 | C2–C1–H7 | 120.2196 | N6-C1-C2-H8 | 179.857 |
| C1–H7 | 1.0862 | N6–C1–H7 | 116.1453 | H7-C1-C2-C3 | 179.8692 |
| C2–C3 | 1.3958 | C1-C2-C3 | 118.9985 | H7-C1-C2-H8 | -0.3121 |
| C2-H8 | 1.0845 | C1-C2-H8 | 120.149 | C2-C1-N6-C5 | -0.0937 |
| C3-C4 | 1.3958 | C3-C2-H8 | 120.8523 | H7-C1-N6-C5 | -179.931 |
| C3-C11 | 1.4986 | C2-C3-C4 | 117.5922 | C1-C2-C3-C4 | 0.0215 |
| C4-C5 | 1.3926 | C2-C3-C11 | 121.1933 | C1-C2-C3-C11 | -179.544 |
| C4-H9 | 1.0845 | C4-C3-C11 | 121.2131 | H8-C2-C3-C4 | -179.796 |
| C5-N6 | 1.3363 | C3-C4-C5 | 118.9968 | H8-C2-C3-C11 | 0.6386 |
| C5-H10 | 1.0862 | C3-C4-H9 | 120.8546 | C2-C3-C4-C5 | -0.0225 |
| C11-Cl12 | 1.8316 | C5-C4-H9 | 120.1484 | C2-C3-C4-H9 | 179.8035 |
| C11-H13 | 1.0876 | C4-C5-N6 | 123.6362 | C11-C3-C4-C5 | 179.5428 |
| C11-H14 | 1.0876 | C4-C5-H10 | 120.2178 | C11-C3-C4-H9 | -0.6311 |
| | | C6-C5-H10 | 116.1458 | C2-C3-C11-Cl12 | -90.1771 |
| | | C1-N6-C5 | 117.1413 | C2-C3-C11-H13 | 151.7184 |
| | | C3-C11-Cl12 | 111.6529 | C2-C3-C11-H14 | 27.9201 |
| | | C3-C11-H13 | 111.9641 | C4-C3-C11-Cl12 | 90.2732 |
| | | C3-C11-H14 | 111.9511 | C4-C3-C11-H13 | -27.8313 |

| | | | | | |
|---|---|---|---|---|---|
| | | Cl12-C11-H13 | 105.5484 | C4-C3-C11-H14 | -151.63 |
| | | C3-C11-H14 | 105.5494 | C3-C4-C5-N6 | -0.036 |
| | | Cl12-C11-H13 | 109.7964 | C3-C4-C5-H10 | -179.869 |
| | | Cl12-C11-H14 | 121.1933 | H9-C4-C5-N6 | -179.863 |
| | | H13-C11-H14 | 121.2131 | H9-C4-C5-H10 | 0.3042 |
| | | | | C4-C5-N6-C1 | 0.0925 |
| | | | | H10-C5-C6-C1 | 179.9313 |

### 3.2 Mullikan and Natural Charge Analysis

These charges influence the dipole moment, polarizability, and other reactive properties of molecules, they are dispersed throughout the atoms and molecular orbital are computed for molecule 4-Chlromethyl pyridine Hydrochloride. The distribution of positive and negative charges surrounding an atom is crucial for increasing or decreasing the bond length between atoms. The findings of two methods for estimating atom charges, Mullikan Population Analysis (MPA) and Natural Atomic Charges (NAC) are listed in the table. 2. The outcome is depicted in a bar graph in Fig. 2.

The carbon atoms C3 in the pyridine ring shows positive (0.081013) NAC value and negative or almost neutral value (-0.04001) MPA value due to the presence of methyl group. In this case NAC prediction is correct compared to MPA. Whereas C5 is attached to the nitrogen atom shows both positive in MPA (0.05993) and NAC (0.205502) due to the electro negative nature of nitrogen atom. In methyl group C11 having less negative MPA (-0.34318) and highly positive (0.465223) NAC because of the attachment of Chlorine atom.

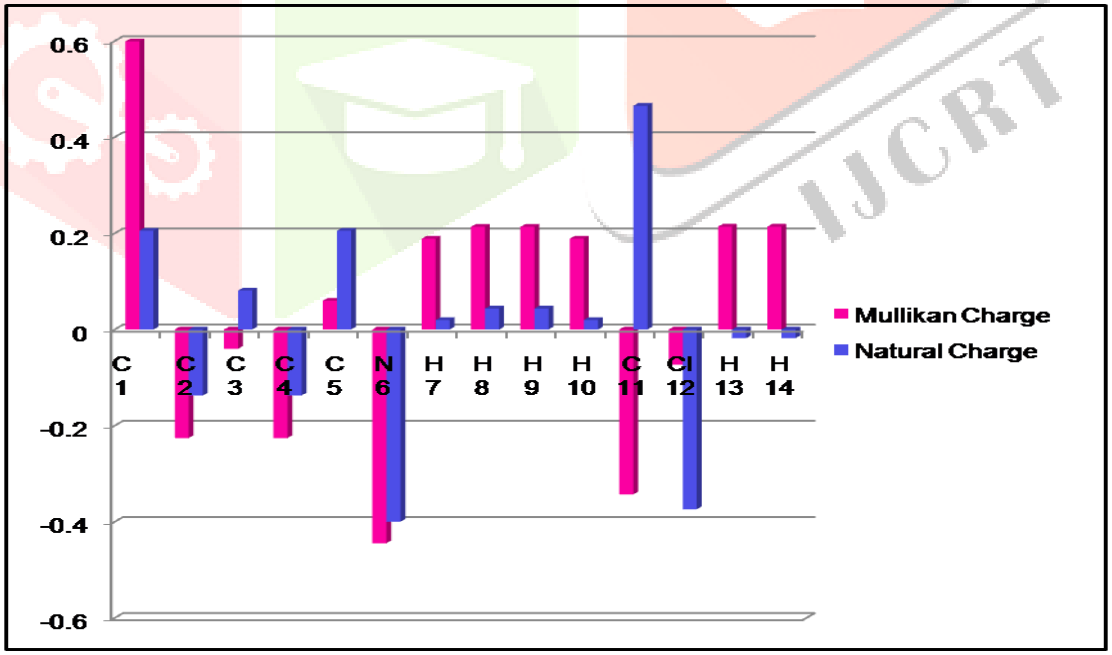


**Fig. 2** Mullikan and Natural Charges bar diagram of 4- Chlromethyl pyridine Hydrochloride

**Table: 2.** Mullikan Charges for 4clmpyhycl Computed at B3LYP/6-311++G (d, p) basis set.

| Atoms | Mullikan Atomic Charge | Natural atomic Charge |
|---|---|---|
| 1C | 0.5991 | 0.205485 |
| 2C | -0.22566 | -0.13723 |
| 3C | -0.04001 | 0.081013 |
| 4C | -0.22567 | -0.1372 |
| 5C | 0.05993 | 0.205502 |
| 6N | -0.44459 | -0.39974 |
| 7H | 0.18881 | 0.019797 |
| 8H | 0.21354 | 0.043675 |
| 9H | 0.21354 | 0.04366 |
| 10H | 0.18881 | 0.019787 |
| 11C | -0.34318 | 0.465223 |
| 12Cl | -0.07329 | -0.37379 |
| 13H | 0.21393 | -0.01809 |
| 14H | 0.21393 | -0.0181 |

### 3.3 NBO Analysis

NBO is extremely useful for analyzing both intermolecular and intra molecular interactions. The energy gap and stabilization energy between them can also be used to understand the various donor and acceptor orbital that are possible in the molecule, as well as the possibility of electronic transitions between them. According to Weinhold's NBO calculation, hyper conjugation has a stabilizing effect that is caused by electrons moving from bonding to antibonding orbital when these molecular orbital are properly orientated.

The donor-acceptor interactions are investigated using a second-order Fock matrix, from which the stabilization E(2) is determined for each donor and acceptor pair, allowing their electronic transitions to be analyzed using the following relationship [11]:

$$E^{(2)} = \Delta E_{ij} = q_i \frac{F(i,j)2}{Ei - Ej}$$

In the aforementioned connection, the stability energy is inversely proportional to the energy gap, so the larger the stabilization energy value, the higher the probability of a transition. The values for each donor and acceptor orbital, as well as their occupancies and stabilization energies, are computed and listed in Table.3. Based on the distance between the donor and acceptor orbital in terms of energy or $E^{(2)}$values in this molecule, the top ten transitions are C3–C4 to C5–N6 ($\pi \rightarrow \pi^*$ 27.53 Kcal/mol), C5–N6 to C1–C2 ($\pi \rightarrow \pi^*$ 26.53 Kcal/mol), C1–C2 to C3–C4 ($\pi \rightarrow \pi^*$ 23.71 Kcal/mol), C 1–C2 to C 5 - N 6 $\pi \rightarrow \pi^*$ 17.56 Kcal/mol), C 3 - C4to C 1 - C 2 ( $\pi \rightarrow \pi^*$ 17.25 Kcal/mol), C5-C6 to C 3 –C 4 ($\pi \rightarrow \pi^*$ 13.6 Kcal/mol), N 6to C 1 – C2 ($n \rightarrow \sigma^*$ 9.23 Kcal/mol), N 6to C 4 – C 5 ($n \rightarrow \sigma^*$ 9.23 Kcal/mol), C 3 –C4 to C11–Cl12 ($\pi \rightarrow \sigma^*$ 6.5 Kcal/mol) and C 1 –H 7to C 5 –N 6 ($\sigma \rightarrow \sigma^*$ 4.72 Kcal/mol). Among these probable transitions of the molecule, the first two transitions are $\pi \rightarrow \pi^*$ transitions, due to the nitrogen atom of the pyridine ring, with considerable high $E^{(2)}$ values, which means these are chemically or biologically the most active sites in the molecule, which coincides with the discussion based on NMR chemical shift values. All the other

transitions in the list are due to then σ →σ* transitions in the pyridine ring, which are almost equally probable and contribute less to the biological properties.

**TABLE 3.** Second-order perturbation theory of Fock matrix in NBO basis of 4- Chlromethyl pyridine Hydrochloride

| DONOR | TYPE OF BOND | OCCUPANCY | ACCEPTOR | TYPE OF BOND | OCCUPANCY | Energy e(2) Kcal/mol | E(j)-e(i) | F(i,j) |
|---|---|---|---|---|---|---|---|---|
| C 3 -C4 | π | 1.63581 | C 5 - N 6 | π* | 0.37198 | 27.53 | 0.27 | 0.077 |
| C 5 - N 6 | π | 1.70738 | C 1 - C 2 | π* | 0.294 | 26.53 | 0.32 | 0.082 |
| C 1 - C2 | π | 1.6295 | C 3 - C4 | π* | 0.34273 | 23.71 | 0.28 | 0.074 |
| C 1 - C 2 | π | 1.6295 | C 5 - N 6 | π* | 0.37198 | 17.56 | 0.27 | 0.061 |
| C 3 - C4 | π | 1.63581 | C 1 - C 2 | π* | 0.294 | 17.25 | 0.29 | 0.064 |
| C 5 - N 6 | π | 1.70738 | C 3 - C 4 | π* | 0.34273 | 13.6 | 0.32 | 0.06 |
| N 6 | n | 1.91741 | C 1 - C2 | σ* | 0.02503 | 9.23 | 0.9 | 0.083 |
| N 6 | n | 1.91741 | C 4 - C 5 | σ* | 0.02504 | 9.23 | 0.9 | 0.083 |
| C 3 - C4 | π | 1.63581 | C11-Cl12 | σ* | 0.03413 | 6.5 | 0.35 | 0.047 |
| C 1 - H 7 | σ | 1.98193 | C 5 - N 6 | σ* | 0.01553 | 4.72 | 1.06 | 0.063 |
| C5 - H10 | σ | 1.98192 | C 1 - N 6 | σ* | 0.01553 | 4.72 | 1.06 | 0.063 |
| C2 - H 8 | σ | 1.97911 | C3 - C 4 | σ* | 0.02463 | 4.34 | 1.1 | 0.062 |
| C 4 - H9 | σ | 1.97911 | C 2 - C 3 | σ* | 0.02462 | 4.34 | 1.1 | 0.062 |
| C2 - H8 | σ | 1.97911 | C1 - N 6 | σ* | 0.01553 | 4.24 | 1.07 | 0.06 |
| C4 - H9 | σ | 1.97911 | C5 - N 6 | σ* | 0.01553 | 4.24 | 1.07 | 0.06 |
| C4 - C 5 | σ | 1.98398 | C3 - C 11 | σ* | 0.02774 | 4.11 | 1.12 | 0.061 |
| C1 - C2 | σ | 1.98398 | C3 - C 11 | σ* | 0.02774 | 4.1 | 1.12 | 0.061 |
| N 6 | n | 1.91741 | C1 - H 7 | σ* | 0.02366 | 4.04 | 0.77 | 0.05 |
| N 6 | n | 1.91741 | C5 - H 10 | σ* | 0.02367 | 4.04 | 0.77 | 0.05 |
| C 11-H14 | σ | 1.98565 | C3 - C4 | σ* | 0.02463 | 3.86 | 1.11 | 0.058 |
| C 11 -H13 | σ | 1.98567 | C2 - C3 | σ* | 0.02462 | 3.85 | 1.11 | 0.058 |
| C 1 - H 7 | σ | 1.98193 | C2 - C3 | σ* | 0.02462 | 3.53 | 1.09 | 0.055 |
| C5 - H 10 | σ | 1.98192 | C3 - C4 | σ* | 0.02463 | 3.53 | 1.09 | 0.055 |
| C2 - C3 | σ | 1.97395 | C3 - C4 | σ* | 0.02463 | 3.48 | 1.28 | 0.06 |
| C3 - C4 | σ | 1.97395 | C2 - C3 | σ* | 0.02462 | 3.48 | 1.28 | 0.06 |
| Cl 12 | n | 1.97291 | C3 - C 11 | σ* | 0.02774 | 3.44 | 0.73 | 0.045 |
| C1 - C2 | σ | 1.98398 | C2 - C3 | σ* | 0.02462 | 3.08 | 1.28 | 0.056 |
| C4 - C5 | σ | 1.98398 | C3 - C4 | σ* | 0.02463 | 3.08 | 1.28 | 0.056 |
| C11 -Cl12 | σ | 1.98111 | C3 - C4 | π* | 0.34273 | 3.01 | 0.65 | 0.043 |
| Cl 12 | n | 1.97851 | C11-H13 | σ* | 0.01701 | 2.88 | 0.7 | 0.04 |
| Cl 12 | n | 1.97851 | C11-H14 | σ* | 0.01702 | 2.88 | 0.7 | 0.04 |
| C2 - C3 | σ | 1.97395 | C1 - C2 | σ* | 0.02503 | 2.66 | 1.28 | 0.052 |
| C3 - C4 | σ | 1.97395 | C4 - C5 | σ* | 0.02504 | 2.66 | 1.28 | 0.052 |
| C2 - C3 | σ | 1.97395 | C4 - H9 | σ* | 0.01369 | 2.65 | 1.14 | 0.049 |
| C3 - C4 | σ | 1.97395 | C2 - H8 | σ* | 0.01369 | 2.65 | 1.14 | 0.049 |
| C1 - N 6 | σ | 1.98655 | C5 - H 10 | σ* | 0.02367 | 2.19 | 1.25 | 0.047 |
| C 5 - N 6 | σ | 1.98656 | C1 - H7 | σ* | 0.02366 | 2.19 | 1.25 | 0.047 |
| C3 - C11 | σ | 1.98436 | C3 - C4 | σ* | 0.02463 | 2.1 | 1.24 | 0.046 |

| | | | | | | | | |
|---|---|---|---|---|---|---|---|---|
| C3 - C11 | σ | 1.98436 | C2 - C3 | σ* | 0.02462 | 2.09 | 1.24 | 0.046 |
| C2 - C3 | σ | 1.97395 | C1 - H7 | σ* | 0.02366 | 1.97 | 1.14 | 0.042 |
| C 3 - C4 | σ | 1.97395 | C5 - H 10 | σ* | 0.02367 | 1.97 | 1.14 | 0.042 |
| C2 - C3 | σ | 1.97395 | C3 - C 11 | σ* | 0.02774 | 1.87 | 1.12 | 0.041 |
| C3 - C4 | σ | 1.97395 | C3 - C 11 | σ* | 0.02774 | 1.87 | 1.12 | 0.041 |
| C3 - C 11 | σ | 1.98436 | C1 - C 2 | σ* | 0.02503 | 1.83 | 1.24 | 0.043 |
| C3 - C11 | σ | 1.98436 | C4 - C5 | σ* | 0.02504 | 1.83 | 1.24 | 0.043 |
| C1 - N6 | σ | 1.98655 | C1 - C2 | σ* | 0.02503 | 1.66 | 1.39 | 0.043 |
| C5 - N6 | σ | 1.98656 | C4 - C5 | σ* | 0.02504 | 1.66 | 1.39 | 0.043 |
| C1 - N6 | σ | 1.98655 | C2 - H8 | σ* | 0.01369 | 1.51 | 1.26 | 0.039 |
| C5 - N6 | σ | 1.98656 | C4 - H9 | σ* | 0.01369 | 1.51 | 1.26 | 0.039 |
| C1 - C2 | σ | 1.98398 | C1 - N6 | σ* | 0.01553 | 1.43 | 1.25 | 0.038 |
| C4 - C5 | σ | 1.98398 | C5 - N6 | σ* | 0.01553 | 1.43 | 1.25 | 0.038 |
| C3 - C4 | σ | 1.97395 | C4 - H9 | σ* | 0.01369 | 1.1 | 1.14 | 0.032 |
| C2 - C3 | σ | 1.97395 | C2 - H8 | σ* | 0.01369 | 1.09 | 1.14 | 0.032 |
| C11 -H 14 | σ | 1.98565 | C3 - C4 | π* | 0.34273 | 1.04 | 0.56 | 0.024 |
| C1 - C2 | σ | 1.98398 | C2 - H8 | σ* | 0.01369 | 0.99 | 1.15 | 0.03 |
| C4 - C5 | σ | 1.98398 | C4 - H9 | σ* | 0.01369 | 0.99 | 1.15 | 0.03 |
| C2 - H8 | σ | 1.97911 | C2 - C3 | σ* | 0.02462 | 0.97 | 1.1 | 0.029 |
| C4 - H9 | σ | 1.97911 | C3 - C4 | σ* | 0.02463 | 0.97 | 1.1 | 0.029 |
| C11 - H13 | σ | 1.98567 | C11-Cl12 | σ* | 0.03413 | 0.96 | 0.63 | 0.022 |
| C 11 -H14 | σ | 1.98565 | C11-Cl12 | σ* | 0.03413 | 0.96 | 0.63 | 0.022 |
| C1 - C2 | σ | 1.98398 | C1 - H7 | σ* | 0.02366 | 0.88 | 1.14 | 0.028 |
| C4 - C5 | σ | 1.98398 | C5 - H 10 | σ* | 0.02367 | 0.88 | 1.14 | 0.028 |
| C1 - N6 | σ | 1.98655 | C5 - N6 | σ* | 0.01553 | 0.85 | 1.36 | 0.03 |
| C3 - C4 | π | 1.63581 | C11-H14 | σ* | 0.01702 | 0.85 | 0.65 | 0.023 |
| C5 - N6 | σ | 1.98656 | C1 - N6 | σ* | 0.01553 | 0.85 | 1.36 | 0.03 |
| C11 -H 13 | σ | 1.98567 | C3 - C4 | π* | 0.34273 | 0.84 | 0.56 | 0.021 |
| Cl 12 | n | 1.97291 | C11-H13 | σ* | 0.01701 | 0.84 | 0.71 | 0.022 |
| Cl 12 | n | 1.97291 | C11-H14 | σ* | 0.01702 | 0.84 | 0.71 | 0.022 |
| Cl 12 | n | 1.97291 | C3 - C4 | π* | 0.34273 | 0.81 | 0.34 | 0.016 |
| C2 - H8 | σ | 1.97911 | C 1 - C2 | σ* | 0.02503 | 0.66 | 1.09 | 0.024 |
| C4 - H9 | σ | 1.97911 | C4 - C5 | σ* | 0.02504 | 0.66 | 1.09 | 0.024 |
| C3 - C4 | σ | 1.97395 | C11-H14 | σ* | 0.01702 | 0.63 | 1.1 | 0.023 |
| C2 - C3 | σ | 1.97395 | C11-H13 | σ* | 0.01701 | 0.62 | 1.1 | 0.023 |

### 3.4 HOMO-LUMO

The chemical stability of a molecule is determined by the number of occupied molecular orbital (HOMO) and the number of unoccupied molecular orbital (LUMO), both of which are referred to as Frontier molecular orbital FMO [12]. The HOMO and LUMO values are proportional to the molecule's ionisation potential and electron affinity. Using the molecule's optimal structure, the energies of LUMO + 3, LUMO + 2, LUMO + 1, LUMO, and HOMO - 3, HOMO - 2, HOMO - 1, HOMO, as well as the associated energy gaps, are calculated. In Fig. 3, the simulated FMOs illustrate the presence of intra molecular charge transfer (ICT) within the molecule and the two-dimensional structure of the energy gaps between HOMO - 3, HOMO - 2, HOMO - 1, HOMO, and LUMO + 3, LUMO + 2, LUMO + 1, LUMO is depicted. The energy band gap is the difference in energy between HOMO and LUMO. The values of global molecular reactivity descriptors like electronegativity (χ), hardness (η), softness (S), and electrophilicity index (ω) anticipated for

the titled molecule are determined by this energy gap. Table. 4 shows that the computed energy of HOMO, HOMO – 1, HOMO – 2, and HOMO – 3 are -0.27404, -0.27618, -0.31000, and -0.32130 eV respectively, and the energies of LUMO, LUMO + 1, LUMO + 2, and LUMO + 3 are -0.00580, 0.00935, 0.00955 and 0.07647eV respectively. The energy gap between HOMO-LUMO is -0.27984 eV. The electronegativity, which is the measure of an atom's attraction to an electron in a covalent bond is 0.13992 eV. The molecules have a chemical hardness of 0.13412 eV and a softness of 0.53648 eV. This molecule is highly reactive because it shows high global softness [13].

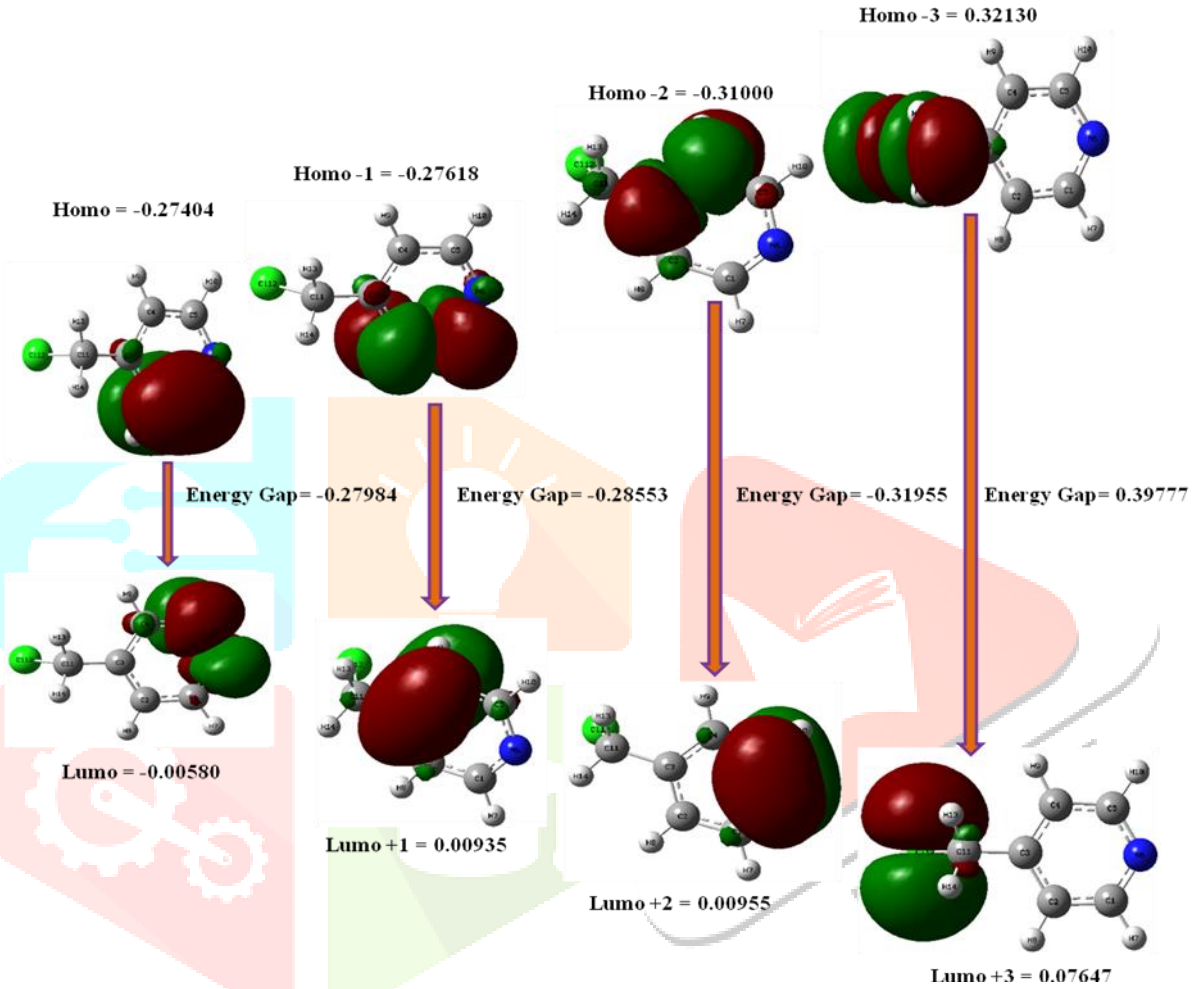


**Fig. 3** Theoretically predicted HOMO- LUMO picture of 4- Chlromethyl pyridine Hydrochloride

**Table 4** HOMO, LUMO, global electronegativity, global hardness and softness, global electrophilicity index of 4clmpyhycl

| **Parameters** | **Gas** |
|---|---|
| $E_{HOMO}$ (ev) | -0.27404 |
| $E_{LUMO}$ (ev) | -0.00580 |
| $\Delta E_{HOMO\text{-}LUMO\ gap}$ (ev) | -0.27984 |
| Electronegativity ($\chi$) | 0.13992 |
| Global hardness ($\eta$) | 0.13412 |
| Global softness (S) | 0.53648 |
| Electrophilicity Index($\omega$) | 0.07298 |

### 3.5 Molecular Electrostatic Potential (MEP)

In terms of colour grading, the MEP displays molecular size, shape, as well as positive, negative, and neutral electrostatic potential regions, and is highly valuable in molecular structure study with its physicochemical property relationship [14]. Potential mapping knowledge of electron density across the molecule is provided by molecular electrostatics. This provides a full description of the intermolecular interaction of in the compound with aims by indicating electron density in different sections of the molecule such as electrophilic and nucleophilic bases in the mixture. The MEPs generally exhibit a blue colour for the maximum positive region, which prefers the location for nucleophilic attack symptoms, and a red colour for the maximum negative region, which prefers the site for electrophilic attack symptoms. In the region with the MEPs, the values of the electrostatic potential at the surface are shown by different colours (from red to blue) for varied data (from the maximum negative to a positive value).The colour of the potential changes from red to blue. In Fig.4, the hues in the titled compound line up between -4.505e-2 (dark red) and 4.505e-2 (dark blue). Blue and red were used to depict the strongest attraction and repulsion, respectively. The MEP map shows that the spots with negative potential are nitrogen atoms (6N). The negative region of these results clearly demonstrates the compound's biological action.

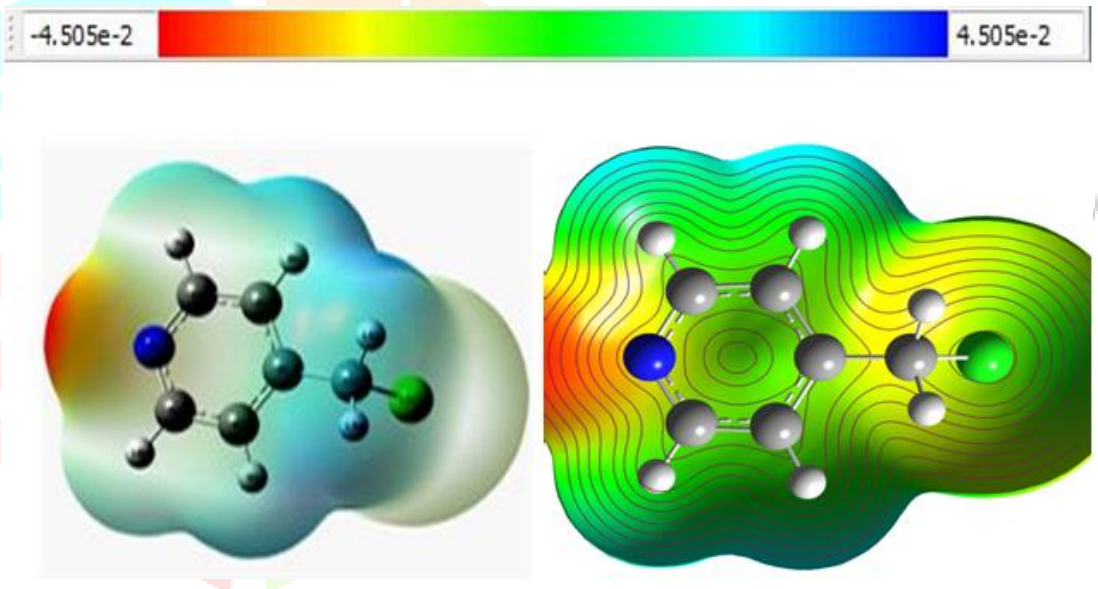


**Fig. 4** Map indicating the electrostatic potential of 4- Chlromethyl pyridine Hydrochloride

### 3.6 Drug likeness

The compound 4-Chlromethyl pyridine Hydrochloride's pharmaceutical potential was estimated and analysed using commonly used drug likeness parameters and molecular docking procedures. Drug similarity factors are extremely useful for estimating the early pharmacokinetic features required for medication distribution success, even if they cannot predict whether a given molecule will exhibit biologically active or not [4,15]. Using Lipinski, Ghose and Veber's rule, the drug likeness of a titled compound is investigated. The following drug similarity metrics are commonly used for the initial assessment of pharmacokinetic qualities: MlogP, number of hydrogen bond donors and acceptors (HBD and HBA, respectively), number of rotatable bonds, total polar surface area (TPSA), and molar refractivity. The computed values are listed in the Table.5. The radar diagram of the drug and the pie chart for the drug likeness are shown in Fig.5. If a chemical is to be used as an oral medication, it should not have hydrogen bond donor values greater than 5

or hydrogen bond acceptor values greater than 10. This molecule has a donor value of zero and an acceptor value of two. Another Lipinski criterion states that the Octanal-Water Purification Factor LogP of a good medicinal molecule should not be greater than 5. It is only found in the current molecule at 1.15. According to the final Lipinski rule, the molecular mass should not be greater than 500 Dalton. In this case, the molecular weight is only 127.57 g/mol. As a result, the current molecule 4- Chlromethyl pyridine Hydrochloride meets all Lipinski criteria.

According to the Ghose rule, a molecule's molecular refractivity should be between 40 and 130, and its atom count should be between 20 and 70. The current molecule is made up of only 14 atoms and has a refractivity of 34. Veber's rule states that a molecule should not have more than ten rotatable bonds, but there are only one in this case. The molecule has a surface area of 12.89 Å². As a result, it can be concluded that the current molecule, 4- Chlromethyl pyridine Hydrochloride, meets all of the requirements for a superior oral drug.

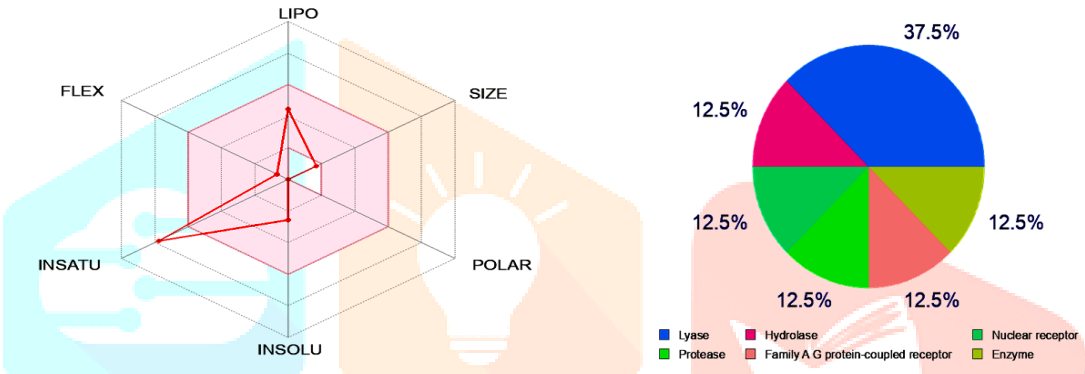


**Fig.5** Radar Diagram of the drug and pie chart for druglikeness

**Table 5** The computed values for drug likeness

| Drug likeness parameters | Values |
|---|---|
| Number of Hydrogen bond donor (HBD) | 0 |
| Number of Hydrogen bond acceptor (HBA) | 1 |
| Number of Rotatable bond | 1 |
| Topological polar surface area(TPSA) | 12.89 Å² |
| Molecular Exact mass | 127.57 g/mol |
| Molar Refractivity | 34 |
| Number of Heavy atom | 8 |
| Number of aromatic heavy atoms | 6 |
| MLogP | 1.15 |

### 3.6.1.Molecular Docking:

Molecular docking is an effective technique for anticipating the molecular mechanism of protein-ligand interactions which include binding to a receptor with known three-dimensional structures [15,16]. Auto Dock 1.5.6 has been used to get inside into probable protein-ligand interactions and to identify the binding affinity of the molecules. Lamackian Genetic Algorithm (LGA) is used for molecular docking analysis. The binding protein from target proton was specified of grid size 90 x 90 x 90Å with the aid of

Autogrid. Table .6, shows the list of the docking results, including residues, hydrogen bonds, and the total number of bonds. The binding pose for the titled compound is illustrated in Fig.6. The ligand was docked into the functional site of the respective protein and its docking energy was examined to get a minimum value. Ligand was docked at active site 1HD2 of receptor. 1HD2 is a Human peroxiredoxin 5, More than 40 antioxidant enzymes in the peroxiredoxin family have evolved to be stable across a wide range of organisms, including bacteria, yeasts, protozoa, plants, and vertebrates. Peroxiredoxins work in collaboration with other antioxidant enzymes and non-enzymatic antioxidants to regulate the levels of reactive oxygen species (ROS) in cells and tissues and protect them from oxidative damage. Peroxiredoxin 5 (PRDX5), also known as PrxV/AOEB166/PMP20, is an unique antioxidant enzyme capable of inhibiting that is widely expressed in mammalian tissues. Peroxiredoxin can be directed intracellularly to the cytosol, peroxisomes, and mitochondria, implying that it may play an important antioxidant role in these major ROS-producing organelles, peroxisomes and mitochondria, as well as in the regulation of signal transduction given its location in the cytosol. The Protein 1HD2 is docked at bond residue LEU 96 at a distance 3.0 Ǻ.

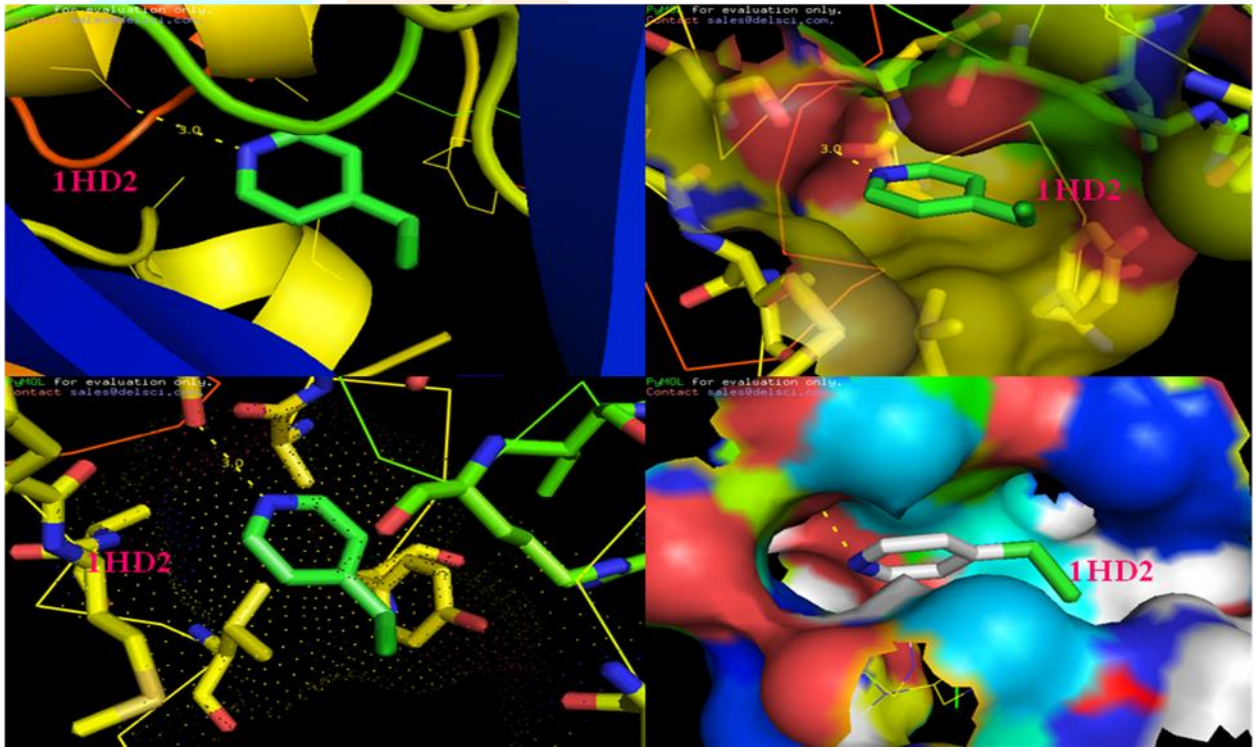


**Fig.6** Binding pose of 4- Chlromethyl pyridine Hydrochloride

**Table 6** The Docking analysis binding pose of 4- Chlromethyl pyridine Hydrochloride

| Sl. No. | Parameter | Result |
|---|---|---|
| 1. | Compound name | 4-Chloromethyl pyridine hydrochloride |
| 2. | Protein ID | 1HD2 |
| 3. | Bond Residue | LEU 96 |
| 4. | Distance (**Å**) | 3.0 |
| 5. | RMSD | 61.952 **Å** |
| 6. | Binding energy | -3.40 kcal/mol |
| 7. | Inhibition constant $k_i$ | 3.20 mM |
| 8. | Total internal energy | -0.11 kcal/mol |
| 9. | Intermolecular energy | -3.70 kcal/mol |
| 10. | Vdw + Hbond + desolv energy | -3.65 kcal/mol |
| 11. | Electrostatic energy | -0.05 kcal/mol |
| 12. | Torsional energy | 0.30 kcal/mol |
| 13. | Ligand efficiency | -0.5 |
| 14. | Unbound energy | -0.11 kcal/mo |
| 15. | Cavity size | 335 |

### 3.6.2 RAMACHANDRA PLOT

The Ramachandran plot is one method of identifying the protein's favorable regions for docking with ligand by examining the distribution of torsion angles in the protein structure. It depicts the dihedral angles of the amino acid residues in a protein in two dimensions. They are useful when using the PASS online predictor to select proteins for docking studies. The Ramachandran plot represented the protein discovered through docking analysis. The protein is identified through docking analysis, the Ramachandran plot with bioavailability of the molecule and the chart was created. The diagram is illustrated in Figures 7. The red area of the diagram represents the advantageous region where the angles of amino acid residues are flexible. The prohibited zones are denoted in black. The figure clearly shows that for the designated protein, a larger proportion of residues and a smaller proportion of residues appear within the permitted red and forbidden regions, respectively. The Ramachandran plot's conclusion supports the preferred proteins of 1HD2 has a structurally viable for docking and drug design.

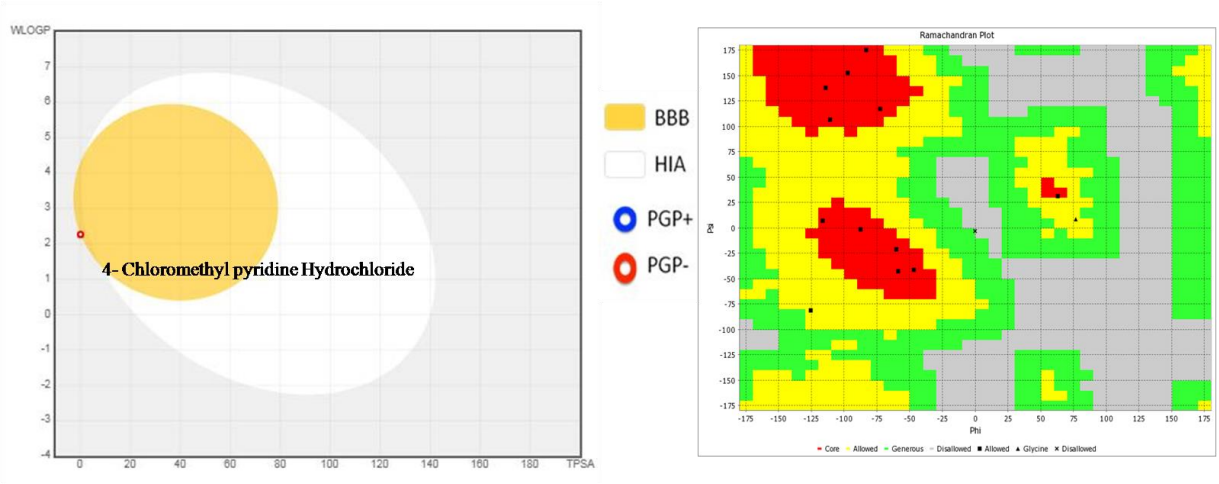


**Fig.7** Bioavailability of 4-BromoMethyl(Benzonitrile) & Ramachandra plot

## IV. Discussion

### 4.1. $^{1}H$ and $^{13}C$ NMR chemical shift

The Table.3 shows experimental and theoretical values for the titled compound's Carbon ($^{13}C$) and Proton ($^{1}H$) NMR. The experimental $^{13}C$ and $^{1}H$ NMR data were recorded in DMSO (Dimethyl Sulfoxide) solvent and are shown in Fig.8. Chemical shift values in both gaseous and liquid phases are shown in Table 7. The GIAO (Gauge Invariant Atomic Orbital) method is used to calculate the theoretical $^{13}C$ and $^{1}H$ chemical transformation for the optimal geometry. In the case of the Pyridine ring, the values 1C, 3C, and 5C are highly deshielded. The deshielded value in 1C (153 ppm) and 5C (153 ppm) results from the electronegative nature of the Nitrogen atom, while 3C is attached to the methyl group. Because of the presence of a chlorine atom and a pyridine ring on either side, the chemical shift of aliphatic chain 11C is shielded (77.36 ppm). The aromatic hydrogen atoms are within the expected range. However, the aliphatic chain 13H and 14H values (4.96 and 4.71 ppm) decrease due to the attachment of the chlorine atom in the titled molecule.

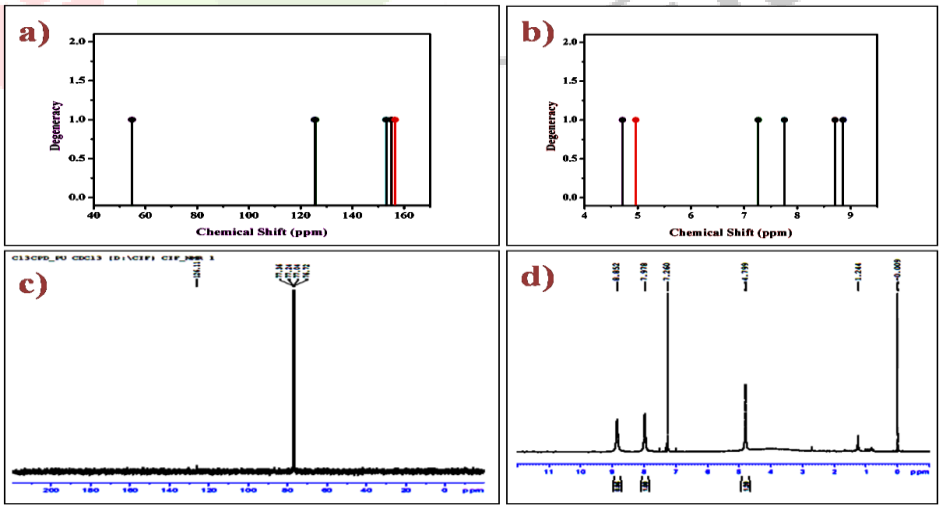


**Fig. 8** a), b) Theoretical and c), d) Experimental $^{13}$ C and $^{1}$H NMR spectra for 4- Chlromethyl pyridine Hydrochloride

**Table. 7.** Calculated both $^{1}H$ and $^{13}C$ NMR Chemical shifts (ppm) of 4clmpyhycl

| **Atom** | **Gas B3LYP/6-311++G(d,p)GIAO (ppm)** | **$CDCl_3$ B3LYP/6-311++G(2d,p)GIAO (ppm)** | **Experimental $CDCl_3$** |
|---|---|---|---|
| 1C | 155.124 | 155.106 | 153 |
| 2C | 124.219 | 125.633 | 126.11 |
| 3C | 151.379 | 153.06 | 153 |
| 4C | 125.078 | 125.516 | 126.11 |
| 5C | 156.769 | 156.422 | 153 |
| 11C | 54.2714 | 54.8591 | 77.36 |
| 7H | 8.7104 | 8.7104 | 8.852 |
| 8H | 6.9991 | 7.2638 | 7.260 |
| 9H | 7.6758 | 7.7576 | 7.978 |
| 10H | 8.881 | 8.8576 | 8.852 |
| 13H | 4.7952 | 4.96344 | 4.799 |
| 14H | 4.5049 | 4.7146 | 4.799 |
| 7H | 8.7104 | 8.7104 | 8.852 |
| 8H | 6.9991 | 7.2638 | 7.260 |

### 4.2 Vibrational Assignments

All of the fundamental vibrational frequencies were calculated and empirically observed. The calculated frequencies were scaled with the suggested scaling factor, and the results were compared to the experimental values. The selected molecule has 14 atoms and 36 fundamental modes, all of which may be recognised in the IR and Raman spectrum. Theoretically computed FT-Raman and FT-IR spectra for the molecule are shown in Fig.9. The Calculated Vibrational frequencies are listed in Table.8

#### 4.2.1 CH Vibrations

In phenyl rings, the CH fundamental frequencies are usually in the range of 3100 to 3000$cm^{-1}$, and they indicate the ring's aromatic character. CH vibrations in the pyridine ring have been seen in this molecule at 3180, 3177, 3158, 3154 $cm^{-1}$ in FT-IR and 3136, 3133, 3110, 3105 $cm^{-1}$ in FT-Raman, with estimated values of 3134, 3133, 3111, and 3108 $cm^{-1}$. Because of the chloromethyl group and the presence of a Nitrogen atom in the pyridine ring, these values are greater than expected. A similar range of 3000-2900 $cm^{-1}$ is expected for the aliphatic chain. However, the FT-IR values are 3054, 2960 $cm^{-1}$, the FT-Raman values are 3100, 3090, 3052 $cm^{-1}$, and the computed values are 3106, 3052 $cm^{-1}$. Several results are higher than expected due to the presence of the N atom [8].

### 4.2.2 CC Vibrations

CC double bonds should be between 1600 and 1500 $cm^{-1}$ in diameter, while single bonds should be between 1500 and 1400 $cm^{-1}$ [9]. Stretching vibrations of the CC type were identified in this molecule at 1612, 1423, 1267, 1229, and 840 $cm^{-1}$. Then the titled molecule having 1630, 1402, 1274, 1236, 867$cm^{-1}$,and 1640, 1444, 1277, 1253, 857 $cm^{-1}$ respectively, are the experimental CC vibrations of FT-IR and FT-Raman. These lower numbers demonstrate that N atom affects these modes.

### 4.2.3 CN Vibrations

The frequency of the C-N bond stretching vibrational mode is generally combined with other vibrational modes and can be found in the wave number in the range of 1382 - 1266 $cm^{-1}$ [10]. The computed values for 1582 and 996 $cm^{-1}$ are revealed in this molecular analysis. In FT-IR and FT-Raman, the experimental CN stretching vibration was observed at 1591, 1057 $cm^{-1}$ and 1621, 1014 cm-1, respectively. Because of the electronegative character of the Nitrogen atom, the readings are greater and lower than expected.

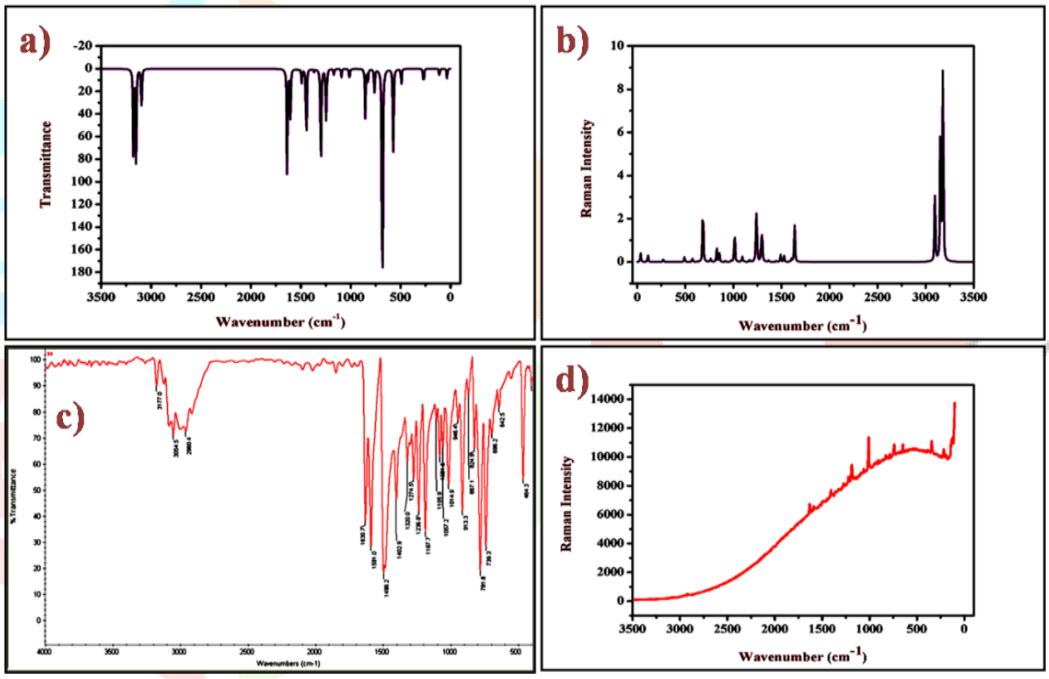


**Fig.9** a), b) Theoretical and c), d) Experimental (FT-IR and RAMAN) spectra for 4- Chlromethyl pyridine Hydrochloride

**Table: 8.** Observed method B3LYP/6-311++G (d, p) level calculated Vibrational frequencies of 4clmpyhycl

| **Experimental frequency ($cm^{-1}$)** | | **B3LYP/6-311++G (d,p)** | | **PED %** |
|---|---|---|---|---|
| ***FT-IR*** | ***FT-RAMAN*** | ***Unscaled ($cm^{-1}$)*** | ***Scaled ($cm^{-1}$)*** | |
| 3180 | 3136 | 3179 | 3134.494 | ν CH45 |
| 3177 | 3133 | 3178 | 3133.508 | ν CH45 |
| 3158 | 3110 | 3156 | 3111.816 | ν CH48 |
| 3154 | 3105 | 3153 | 3108.858 | νCH43 |
| 3054 | 3100 | 3151 | 3106.886 | ν CH45 |
| 2960 | 3090 | 3096 | 3052.656 | ν CH50 |
| 1630 | 1640 | 1635 | 1612.11 | ν CC17 |
| 1591 | 1621 | 1605 | 1582.53 | ν NC25 |
| | 1521 | 1524 | 1502.664 | β HCN24 |
| 1496 | 1483 | 1489 | 1468.154 | β HCH93 |
| 1402 | 1444 | 1444 | 1423.784 | ν CC13 |
| 1320 | 1373 | 1365 | 1345.89 | β HCN21 |
| | 1292 | 1297 | 1278.842 | γ CHCH98 |
| 1274 | 1277 | 1286 | 1267.996 | ν CC18 |
| 1236 | 1253 | 1247 | 1229.542 | ν CC14 |
| | 1229 | 1236 | 1218.696 | β HCC11 |
| 1187 | 1157 | 1167 | 1150.662 | β HCC75 |
| 1105 | 1100 | 1108 | 1092.488 | β HCC12 |
| 1081 | 1086 | 1092 | 1076.712 | β HCC21 |
| 1057 | 1014 | 1011 | 996.846 | ν NC19 |
| 1014 | 1009 | 1001 | 986.986 | γ CCNH37 |
| 946 | 976 | 979 | 965.294 | γ CCNH33 |
| 913 | 909 | 918 | 905.148 | ν CC10 |
| | 890 | 881 | 868.666 | τ HCCN34 |
| 867 | 857 | 852 | 840.072 | ν CC10 |
| 824 | 828 | 826 | 814.436 | ν CC21 |
| 781 | 770 | 761 | 750.346 | τ HCCN19 |

| | | | | |
|---|---|---|---|---|
| 696 | 670 | 683 | 673.438 | ν CC10 |
| 642 | 658 | 682 | 672.452 | ν ClC58 |
| | 579 | 572 | 563.992 | β CCC27 |
| 464 | 493 | 491 | 484.126 | ν CC10 |
| | 383 | 383 | 377.638 | τ CNCC15 |
| | 307 | 325 | 320.45 | β CCC80 |
| | 273 | 269 | 265.234 | ν ClC10 |
| | 111 | 110 | 108.46 | τ CCCC62 |
| | | 34 | 33.524 | τ CCCCl98 |

**4.3 UV-Visible Analysis**

As illustrated in Fig. 10, the titled molecule has a chloromethyl functional group linked to the Pyridine ring. The change in charge distribution at the molecular orbitals at the sites 5C-6N & 1C-6N, where the N atom is embedded in the benzene ring, forming a Pyridine ring, and at 3C-11C, where the Cl is attached to the methyl group, is expected to cause changes in the structural, physico-chemical, and biological properties of the molecule. Theoretical electronic absorption spectra of 4-Cholоromethyl pyridine hydrochloride is calculated in Table.9.

According to the UV table, the major electronic transitions can happen at wavelengths 261, 245, 230,206, 197, 195, 192, 188, 187 nm in gas phase, and at wavelenths 251, 235, 230, 206, 194, 193, 187.7 and 187.4nm correspondingly in solvent- ethanol phase. 0.0042, & 0.0000 0.0322, 0.0119, 0.0048, 0.0075, 0.0659, 0.0029, 0.0045, 0.0810 are the oscillator strengths that show peak intensity in the UV spectrum for the gas phase ten transitions in the appropriate order.The first two transitions, 0.0042 and 0.0000, imply that they will be faint and not visible in the spectrum. The third, seventh, and tenth transitions, with oscillator strengths of 0.0322, 0.0659, and 0.0810, imply that they will be quite prominent in the spectrum, whereas the first two, with wavelengths of 230 and 195 nm, are owing to transitions between adjacent CC bonds in the pyridine ring. The last one, at 187 nm, could be caused by transitions near the N atom in the pyridine ring. The oscillator strengths in the solvent phase are 0.0051, 0.0001, 0.0508, 0.0212, 0.0852, 0.0599, 0.1437, 0.0079, 0.0409, 0.067, indicating that only the third, fifth, and seventh transitions will be visible in the UV spectrum at wavelengths of 230, 194, and 187 nm, respectively. The bonds involved are identical to those observed in the gas phase. However, the experimental spectrum presented in Fig.6 reveals two notable peaks at 283, 243 nm, the first is definitely an π- σ* transition, which must be focused on the N atom in the pyridine ring, and the second is due to the π – π* transition, which is theoretically expected around 230 nm.

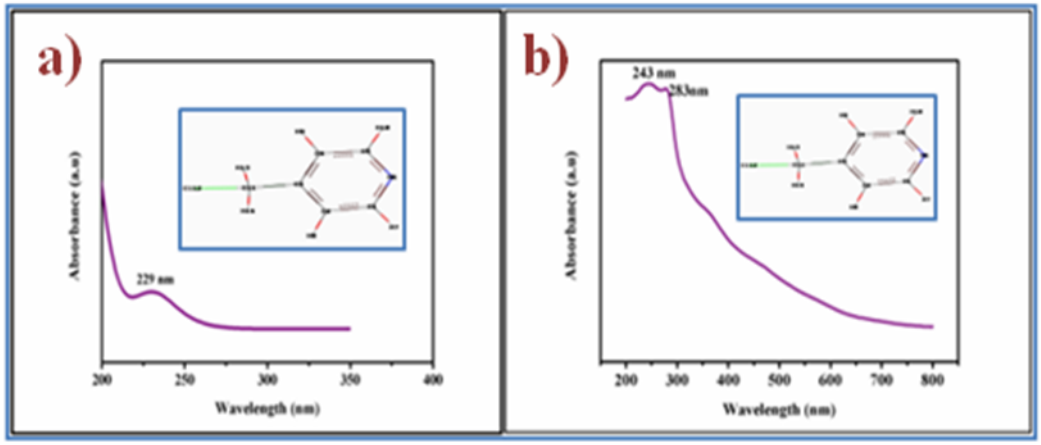


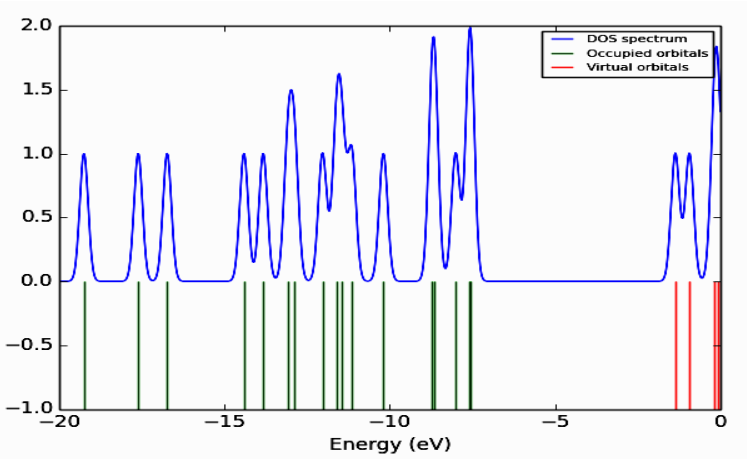


**Fig.10** a) Theoretical and b) Experimental UV-visible spectra for 4- Chlromethyl pyridine Hydrochloride

**Table: 9.** Theoretical electronic absorption spectra of 4clmpyhycl absorption wavelength λ (nm), excitation energies E (eV) and oscillator strengths (f) using TD-DFT/B3LYP/6-311++G (d, p) method.

| λ (nm) | Experimen-tal value | E(eV) | (f) | Major contribution |
|---|---|---|---|---|
| **GAS** | | | | |
| 261.15 | | 4.7476 | 0.0042 | HOMO->LUMO (98%) |
| 245.46 | | 5.0511 | 0.0000 | HOMO->LUMO+1 (99%) |
| 230.33 | | 5.3829 | 0.0322 | HOMO-1->LUMO (73%) |
| 206.23 | | 6.0119 | 0.0119 | HOMO-2->LUMO (64%) |
| 197.06 | | 6.2917 | 0.0048 | HOMO->LUMO+2 (65%) |
| 195.63 | | 6.3378 | 0.0075 | HOMO-3->LUMO (66%) |
| 193.54 | | 6.4062 | 0.0659 | HOMO-4->LUMO (61%) |
| 192.54 | | 6.4394 | 0.0029 | HOMO-1->LUMO+2 (94%) |
| 188.35 | | 6.5825 | 0.0045 | HOMO->LUMO+3 (87%) |
| 187.42 | | 6.6155 | 0.0810 | HOMO-2->LUMO+1 (48%) |
| **solvent** | | | | |
| 251.5 | 243 | 4.9298 | 0.0051 | HOMO->LUMO (88%) |
| 285.31 | 283 | 5.2689 | 0.0001 | HOMO->LUMO +1 (87%) |
| 230.83 | | 5.3712 | 0.0508 | HOMO-1->LUMO (68%) |
| 206.79 | | 5.9955 | 0.0212 | HOMO-2->LUMO (66%) |
| 194.84 | | 6.3635 | 0.0852 | HOMO-3->LUMO (55%) |
| 193.26 | | 6.4155 | 0.0599 | HOMO-4->LUMO (50%) |
| 187.73 | | 6.6044 | 0.1437 | HOMO-2->LUMO+1 (57%) |
| 187.42 | | 6.6153 | 0.0079 | HOMO-1->LUMO+2 (46%) |
| 186.62 | | 6.6436 | 0.0409 | HOMO-1->LUMO+2 (44%) |

| | | | | |
|---|---|---|---|---|
| 183.9 | | 6.7418 | 0.067 | HOMO-1->LUMO+3 (27%) |

## V. CONCLUSION

The bond angles are in the $sp^2$ and $sp^3$ hybridization. The Natural Population Analysis Charge (NAC) prediction is correct compared to Mullikan Population Analysis (MPA). Whereas C5 is attached to the nitrogen atom shows both positive in MPA (0.05993) and NAC (0.205502) due to the electro negative nature of nitrogen atom. In methyl group C11 having less negative MPA (-0.34318) and highly positive (0.465223) NAC because of the attachment of Chlorine atom. The aromatic hydrogen atoms are within the expected range. However, the aliphatic chain 13H and 14H values decreased due to the attachment of the chlorine atom in the titled molecule. The titled molecule constitutes the three types of stretching modes, C-C, C-H, C-N vibrational are differ from the excepted range, because of the electronegative character of the Nitrogen atom, the readings are greater and lower than expected. In NBO analysis, the most probable transitions of the molecule are $\pi \rightarrow \pi^*$ transitions, due to the nitrogen atom of the pyridine ring. In UV-Visible analysis, the enhanced experimental UV absorption at 243nm and 283nm due to $\pi \rightarrow \pi^*$ transition in the pyridine ring, due to CN the $\pi$ and $\pi^*$ orbitals, can be considered as an indicator to the enhanced biological activities of the molecule.

## VI. ABBREVIATIONS

XRD X-ray diffraction
DFT Density Function Theory
NMR Nuclear Magnetic Resonance
FTIR Fourier-transform infrared spectroscopy
NBO Natural Bonding Orbital
HOMO Highest Occupied Molecular Orbital
LUMO Lowest Unoccupied Molecular Orbital
MEP Molecular Electrostatic Potential

## VII. ACKNOWLEDGMENT

The authors would like to express their gratitude to Pondicherry University's Central Instruments Facility for providing the instrumentation.

## REFERENCES

**Journals:**

[1] T.-L. Ho, M. Fieser, L. Fieser, 4-Picolyl chloride hydrochloride, Fieser Fieser's Reagents Org. Synth. (2006) 3971. https://doi.org/10.1002/9780471264194.fos08300.

[2] S. Tighadouini, R. Benabbes, M. Tillard, D. Eddike, K. Haboubi, K. Karrouchi, S. Radi, Synthesis, crystal structure, DFT studies and biological activity of (Z)-3-(3-bromophenyl)-1-(1,5-dimethyl-1H-pyrazol-3-yl)-3-hydroxyprop-2-en-1-one, Chem. Cent. J. 12 (2018) 1–11. https://doi.org/10.1186/s13065-018-0492-

4.

[3] Y. Liu, J. Zhang, T. Feng, Y. Li, Synthesis, structure-fluorescence relationships and density functional theory studies of novel naphthalimide-piperazine-pyridine-based polystyrene sensors for Hg(ii) detection, RSC Adv. 10 (2020) 25281–25289. https://doi.org/10.1039/d0ra04557h.

[4] F. Akman, K. Sarac, Molecular structure, vibration properties and quantum chemical calculations of 4-(chloromethyl)-7-methoxycoumarin and 4-(chloromethyl)-7-methyl-coumarin, Nat. Sci. Discov. 2 (2016) 2–9. https://doi.org/10.20863/nsd.78025.

[5] K.M. Al-Ahmary, M.M. Habeeb, S.H. Aljahdali, Synthesis, spectroscopic studies and DFT/TD-DFT/PCM calculations of molecular structure, spectroscopic characterization and NBO of charge transfer complex between 5-amino-1,3-dimethylpyrazole (5-ADMP) with chloranilic acid (CLA) in different solvents, J. Mol. Liq. 277 (2019) 453–470. https://doi.org/10.1016/j.molliq.2018.12.072.

[6] A.O. Zacharias, A. Varghese, K.B. Akshaya, M.S. Savitha, L. George, DFT, spectroscopic studies, NBO, NLO and Fukui functional analysis of 1-(1-(2,4-difluorophenyl)-2-(1H-1,2,4-triazol-1-yl)ethylidene) thiosemicarbazide, J. Mol. Struct. 1158 (2018) 1–13. https://doi.org/10.1016/j.molstruc.2018.01.002.

[7] O. Noureddine, S. Gatfaoui, S.A. Brandan, A. Sagaama, H. Marouani, N. Issaoui, Experimental and DFT studies on the molecular structure, spectroscopic properties, and molecular docking of 4-phenylpiperazine-1-ium dihydrogen phosphate, J. Mol. Struct. 1207 (2020) 127762. https://doi.org/10.1016/j.molstruc.2020.127762.

[8] S. Sevvanthi, S. Muthu, M. Raja, S. Aayisha, S. Janani, PES, molecular structure, spectroscopic (FT-IR, FT-Raman), electronic (UV-Vis, HOMO-LUMO), quantum chemical and biological (docking) studies on a potent membrane permeable inhibitor: dibenzoxepine derivative, Heliyon. 6 (2020) e04724. https://doi.org/10.1016/j.heliyon.2020.e04724.

[9] M.S. Almutairi, K. Jayasheela, S. Periandy, A.R. Al-Ghamdi, S. Sebastian, S. Xavier, A.A. Kadi, A.S. Abdelhameed, M.I. Attia, Structural, spectroscopic, Hirshfeld surface and charge distribution analysis of 3-(1H-imidazole-1-yl)-1-phenylpropan-1-ol complemented by molecular docking predictions: An integrated experimental and computational approach, J. Mol. Struct. 1196 (2019) 578–591. https://doi.org/10.1016/j.molstruc.2019.07.003.

[10] K. Jayasheela, L.H. Al-Wahaibi, S. Periandy, H.M. Hassan, S. Sebastian, S. Xavier, J.C. Daniel, A.A. El-Emam, M.I. Attia, Probing vibrational activities, electronic properties, molecular docking and Hirshfeld surfaces analysis of 4-chlorophenyl ({[(1E)-3-(1H-imidazol-1-yl)-1-phenylpropylidene]amino}oxy)methanone: A promising anti-Candida agent, J. Mol. Struct. 1159 (2018) 83–95. https://doi.org/10.1016/j.molstruc.2018.01.042.

[11] R. Yankova, S. Genieva, G. Dimitrova, Molecular structure, vibrational, HOMO-LUMO, MEP and NBO analysis of hafnium selenite, J. Mol. Struct. 1141 (2017) 668–677. https://doi.org/10.1016/j.molstruc.2017.04.004.

[12] K. Govindarasu, E. Kavitha, Vibrational spectra, molecular structure, NBO, UV, NMR, first order hyperpolarizability, analysis of 4-Methoxy-4′-Nitrobiphenyl by density functional theory, Spectrochim. Acta - Part A Mol. Biomol. Spectrosc. 122 (2014) 130–141. https://doi.org/10.1016/j.saa.2013.10.122.

[13] S. Aayisha, T.S. Renuga Devi, S. Janani, S. Muthu, M. Raja, R. Hemamalini, Structural (PES), AIM, spectroscopic profiling (FT-IR, FT-Raman, NMR and UV), HOMO-LUMO and docking studies of 2,2-dimethyl-N-(2-pyridinyl)propanamide – a DFT approach, Chem. Data Collect. 24 (2019) 100287. https://doi.org/10.1016/j.cdc.2019.100287.

[14] M. Raja, R. Raj Muhamed, S. Muthu, M. Suresh, Synthesis, spectroscopic (FT-IR, FT-Raman, NMR, UV–Visible), NLO, NBO, HOMO-LUMO, Fukui function and molecular docking study of (E)-1-(5-bromo-2-hydroxybenzylidene)semicarbazide, J. Mol. Struct. 1141 (2017) 284–298. https://doi.org/10.1016/j.molstruc.2017.03.117.

[15] M.H. Rahuman, S. Muthu, B.R. Raajaraman, M. Raja, H. Umamahesvari, Investigations on 2-(4-Cyanophenylamino) acetic acid by FT-IR,FT-Raman, NMR and UV-Vis spectroscopy, DFT (NBO, HOMO-LUMO, MEP and Fukui function) and molecular docking studies, Heliyon. 6 (2020) e04976. https://doi.org/10.1016/j.heliyon.2020.e04976.

[16] C.S. Abraham, S. Muthu, J.C. Prasana, S.J. Armaković, S. Armaković, F. Rizwana B., B.G. Ben, Spectroscopic profiling (FT-IR, FT-Raman, NMR and UV-Vis), autoxidation mechanism (H-BDE) and molecular docking investigation of 3-(4-chlorophenyl)-N,N-dimethyl-3-pyridin-2-ylpropan-1-amine by DFT/TD-DFT and molecular dynamics: A potential SSRI drug, Comput. Biol. Chem. 77 (2018) 131–145. https://doi.org/10.1016/j.compbiolchem.2018.08.010.